Predicting Brain Regions Related to Alzheimer's Disease Based on Global Feature

Qi Wang[1,2], Siwei Chen[3], He Wang[4], Luzeng Chen[5], Yongan Sun[3,*], Guiying Yan[1,2,*]

[1]Academy of Mathematics and Systems Science, Chinese Academy of Sciences, Beijing, China.

[2]School of Mathematical Sciences, University of Chinese Academy of Sciences, Beijing, China.

[3]Department of Neurology, Peking University First Hospital, Beijing, China.

[4]Department of Medical imaging, Peking University First Hospital, Beijing, China.

[5]Department of Ultrasound, Peking University First Hospital, Beijing, China.

The first two authors contributed equally to this paper

Abstract

Alzheimer's disease (AD) is a common neurodegenerative disease in the elderly, early diagnosis and timely treatment are very important to delay the course of the disease. In the past, most of the brain regions related to AD were identified based on the imaging method, which can only identify some atrophic brain regions. In this work, we used mathematical models to find out the potential brain regions related to AD. First, diffusion tensor imaging (DTI) was used to construct the brain structural network. Next, we set a new local feature index 2hop-connectivity to measure the correlation among different areas. And for this, we proposed a novel algorithm named 2hopRWR to measure 2hop-connectivity. At last, we proposed a new index GFS (Global Feature Score) based on global feature by combing 5 local features: degree centrality, betweenness centrality, closeness centrality, the number of maximal cliques, and 2hop-connectivity, to judge which brain regions are likely related to Alzheimer's Disease. As a result, all the top ten brain regions in GFS scoring difference between the AD group and the non-AD group were related to AD by literature verification. Finally, the results of the canonical correlation analysis showed that the GFS was significantly correlated with the scores of the mini-mental state examination (MMSE) scale and montreal cognitive assessment (MoCA) scale. So, we believe the GFS can also be used as a new index to assist in diagnosis and objective monitoring of disease progression. Besides, the method proposed in this paper can be used as a differential network analysis method in other areas of network analysis.

Keywords: Alzheimer's disease, diffusion tensor imaging, brain structural network, 2hop-connectivity, global feature score, differential network analysis

1. Introduction

Alzheimer's disease (AD) is a common neurodegenerative disease in the elderly. It is a continuous process from the pre-clinical stage, mild cognitive impairment (MCI) to dementia. Effective intervention in the pre-dementia stage or MCI stage may delay or reverse the process of the disease. Therefore, early identification of AD patients in the pre-dementia stage or MCI stage, as well as early and timely intervention, are very important for the prognosis of patients. With the development of imaging technology, the detection of AD is not limited to the phenomenon of abnormal protein deposition. It may be an effective method for early diagnosis and monitoring of disease progression to analyze brain structural network information, such as brain connectome analysis (Fan *et al.*, 2016).

A previous study (Liu *et al.*, 2017) have shown that the change of topological feature of the brain

structural network is a marker of many kinds of neuropsychiatric diseases. At present, there are some analysis and research work on brain structural networks based on graph theory (Sanz-Arigita *et al.*, 2010; John *et al.*, 2016). The common method is to analyze some local properties such as the degree centrality of nodes, clustering coefficient, and shortest path length of the brain structural network and so on. Local features are difficult to reveal the whole characteristics of the network. In fact, global property by combining local properties can reveal the topological characteristics of the network more effectively, but it is never easy for choosing which local indexes. In this paper, we first defined a new local feature index 2hop-connectivity of the network to analyze the brain network more completely.

In this work, 20 AD patients and 13 pre-dementia stages (non-AD) were recorded. We collected demographic data and clinical data, completed neuropsychological scale evaluation, and DTI scans. After image preprocessing, the brain structural network was constructed based on the number of fibers between different brain regions. The data of the AD group and the non-AD group were analyzed to get the local topological features of the brain structural network. At the same time, we designed an algorithm named 2hopRWR to get the local feature index 2hop-connectivity, and then we proposed a new index GFS by combing four classical local features and 2hop-connectivity. As a result, we predicted and analyzed the top 10 brain regions according to GFS scoring difference between the AD group and the non-AD group. Then, we analyzed the correlation between the GFS and the cognitive scale scores by canonical correlation analysis (CCA). Finally, we discussed the strengths and limitations of our work and its prospects.

2. Materials and methods

2.1 Data collection and pre-processing

In this research, 20 AD patients and 13 healthy control (non-AD) were recorded. We collected demographic data and clinical data, completed neuropsychological scale evaluation (Supplementary materials table 1) and DTI scans. After image preprocessing, the deterministic fiber tracking FACT method was used to construct the brain structural network. We use AAL brain atlas to divide each subject's brain into 45 left and right symmetrical brain regions, 90 brain regions in total. Each node represents a brain region in the brain structural network. The fiber connection between any two brain regions is represented by an edge, and the edge weight represents the fiber number. The fiber number (FN) matrix of 90 brain regions was obtained by PANDA (Pipeline for Analyzing BraiN Diffusion imAges) (Cui *et al.*, 2013).

Mathematically, we regarded 90 brain regions and its fiber connection as a weighted graph $G(V,E,W)$, and $V=\{v_1,v_2,\dots,v_{90}\}$, $E=\left\{e_{v_iv_j}, v_i\neq v_j\right\}$, $W=\left\{w_{v_iv_j}\right\}$, where v_i denotes the i-th brain region, $e_{v_iv_j}$ is the edge if there are fibers connection between brain region v_i and v_j, and $w_{v_iv_j}$ is the edge weight which is the fiber number between brain region v_i and v_j. The average value of the FN matrix of AD is calculated by adding the FN matrix of each AD patient and divided it by the number of AD patients. Similarly, we take the average value of the FN matrix of all normal controls to the FN matrix of the non-AD group.

2.2 Local features

2.2.1 Degree Centrality

Let $d(v_i)$ denote the degree of a node v_i, which is the number of nodes associated with v_i. And the degree centrality of a node v_i as follows:

$$C_D(v_i) = \frac{d(v_i)}{n-1} \quad (1)$$

2.2.2 Betweenness centrality

Betweenness centrality c_B of a node v_i is the sum of the fraction of all-pairs shortest paths that pass through v_i:

$$c_B(v_i) = \sum_{v_s, v_t \in V} \frac{\sigma(v_s, v_t|v_i)}{\sigma(v_s, v_t)} \quad (2)$$

where $\sigma(v_s, v_t)$ is the number of the shortest paths between v_s and v_t, and $\sigma(v_s, v_t|v_i)$ is the number of the shortest paths passing through the node v_i. If $s = t$, $\sigma(v_s, v_t) = 1$, and if $i = s$ or $i = t$, $\sigma(v_s, v_t|v_i) = 0$.

In short, if the shortest path between many nodes in the network passes through a point v, then v has a high degree of betweenness centrality. That is to say, this node is on the shortcut between other node pairs.

2.2.3 Closeness centrality

Closeness centrality C_c of a node v_i is the reciprocal of the sum of the shortest path distances from v_i to all $n-1$ other nodes. Since the sum of distances depends on the number of nodes in the graph, closeness is normalized by $n-1$.

$$C_c(v_i) = (n-1) / \sum_{\substack{j=1 \\ j \neq i}}^{n} d(v_j, v_i) \quad (3)$$

where $d(v_j, v_i)$ is the shortest path distance between v_j and v_i, and n is the number of nodes in the graph.

Closeness centrality is the sum of the distance from a node to all other nodes. The smaller the sum is, the shorter the path from this node to all other nodes is, and the closer the node is to all other nodes. It reflects the proximity between a node and other nodes.

2.2.4 Number of maximal cliques

In graph theory, the clique of graph G is a complete subgraph H of G. H is a maximal clique of graph G if it is not included by any other clique. The number of maximal cliques of a node can reflect the closeness between the node and other nodes. Only when multiple nodes are all connected can they be considered as maximal cliques. In this paper, we use $N_{MC}(v_i)$ to represent the number of maximal cliques for node v_i.

2.2.5 2hop-connectivity

When examining the correlation of any two nodes in the network, most network analysis methods only consider whether there is an edge connection between two nodes, that is, if there is an edge, the correlation is high, and if there is no connection, the correlation is very weak. In this case, if the edge of the graph is missing due to the disturbance, the result may have a large deviation. For example, for the general random walk (RW) algorithm, the state transition probability is determined by the adjacency matrix of the network. If the adjacency matrix is disturbed, its steady-state probability will change. Generally, when analyzing the correlation of network nodes, the correlation of unconnected nodes in the network will be very low, which is difficult to find the potential characteristics of the network. For any different two nodes in the network, to describe the correlation more accurately, this work not only considers the first-order neighbors between nodes, but also the second-order neighbors between nodes, and we propose an algorithm named 2hopRWR. Finally, each node can get a novel local feature index 2hop-connectivity, which numerical size is represented by local feature score S_{2-hop}. The importance of nodes can be judged based on S_{2-hop}, the larger the S_{2-hop}, the more important the node is.

2.2.5.1 2-hop random walk with restart algorithm

The general random walk on the graph is a transition process by moving from a given node to a randomly selected neighboring node for each step. Consequently, we also regard the node-set $\{v_1, v_2, \dots, v_n\}$ as a set of states $\{s_1, s_2, \dots, s_n\}$ in a finite Markov chain $\mathcal{M}$. The transition probability of $\mathcal{M}$ is a conditional probability defined as $P(v_j, v_i) = Prob(s_{t+1} = v_i | s_t = v_j)$ which means that the $\mathcal{M}$ will be at v_i at time $t+1$ given that it was at v_j at time t. $\mathcal{M}$ is homogeneous because the transition probability from one state to another is independent of time t. What is more, for any v_j of V we have $\sum_{v_i \in V} P(v_j, v_i) = 1$. Note that $\mathcal{M}$ is memoryless, therefore, we can define a transition matrix $P \in \mathbb{R}^{|V| \times |V|}$ of $\mathcal{M}$.

Generally, define transition probability $P(v_j, v_i)$ as follows:

$$P(v_j, v_i) = \frac{1}{d(v_j)}, \tag{4}$$

Denote $D_G = diag\{d_1, d_2, \dots, d_n\}$ be the diagonal matrix, where $d_i = \sum_{j=1}^{n} w_{v_i v_j}$. Thus, P can be rewritten in matrix notation as follows:

$$P = D_G^{-1} W. \tag{5}$$

Define $r_t \in \mathbb{R}^{|V| \times 1}$ as a vector in which the i-th element represents the probability of discovering the random walk at node v_i at step t, so the probability r_{t+1} can be calculated iteratively by:

$$r_{t+1} = P^T r_t. \tag{6}$$

For the random walk with restart (RWR) algorithm (Tong *et al.*, 2006 - 2006), there is an additional restart item compared to the above algorithm. The probability r_{t+1} can be calculated iteratively by the following expression:

$$r_{t+1} = cP^T r_t + (1-c) r_0. \tag{7}$$

Define initial probability $r_0 \in \mathbb{R}^{|V| \times 1}$ as a vector in which the i-th element is equal to one, while other elements are zeros. And $1-c$ is the restart probability $(0 \le c \le 1)$.

But RW and RWR algorithms are all based on the 1-hop neighbor relationship, that is, random walk is based on the existing edge of the graph. If some edges of the graph are missing, the corresponding points cannot be directly transferred, which will lead to a large deviation of the steady-state probability. Therefore, the effectiveness of these algorithms is too much dependent on the integrity of the graph structure. Therefore, in this work, besides the 1-hop neighbor relationship, we also consider the 2-hop neighbors and propose a novel random walk algorithm named 2hopRWR.

The probability r_{t+1} can be calculated iteratively by:

$$r_{t+1} = c(\alpha_1 P^T + \alpha_2 (P^2)^T) r_t + (1-c) r_0. \tag{8}$$

where α_1 and α_2 are the percentage of choosing 1-hop neighbors and 2-hop neighbors, respectively. Specifically, for each point $v_i \in V$, α_1 is the ratio of the number of 1-hop neighbors to the total number of 1-hop and 2-hop neighbors, α_2 is the ratio of the number of 2-hop neighbors to the total number of 1-hop and 2-hop neighbors. Therefore, $\alpha_1 + \alpha_2 = 1$.

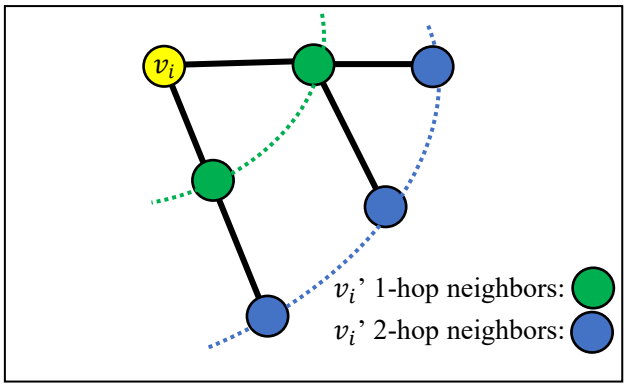

Fig.1 A schematic diagram of 1-hop and 2-hop neighbors

At the beginning of the 2hopRWR, we choose a starting node v_i, then it would have a probability of c to walk to other nodes and also have a probability of $1-c$ to stay in place. Specifically, when the process of walk reaches the node v_j, it has a probability of $\alpha_1 c$ to walk based on existing edges to 1-hop neighbors and has a probability of $\alpha_2 c$ to walk to 2-hop neighbors, and it also has a probability of $1-c$ to restart the walk, that is, to go back to the node v_i.

After some steps, the RWR will be stable, that is, when t tends to infinity, $r_{t+1} = r_t$. The proof is given in Section 2.2.5.2. When the RWR is stable, stable probability between node v_i and node v_j is defined as the j-th element of r_t corresponding to the starting node is v_i.

Input: The weighted adjacency matrix $W = \{w_{v_i v_j}\}$, the restart probability $1-c$, and the starting vector r_0
Output: The ranking vector $\lim_{t\to\infty} r_t$
Step1: Define $D_G = diag\{d_1, d_2, \dots, d_n\}, d_i = \sum_{j=1}^{n} w_{v_i v_j}$.
Step2: Compute and store transition matrix $P = D_G^{-1} W$.
Step3: Define α_1 and α_2. Compute and store α_1 and α_2.
Step4: Output $\lim_{t\to\infty} r_t = (1-c)(I - c(\alpha_1 P^T + \alpha_2 (P^2)^T))^{-1} r_0$.

Fig.2 2hopRWR algorithm framework

2.2.5.2 Proof of convergence

Here we will prove that the random walk with restart algorithm is convergent, that is, for equation (8) when t tends to infinity, $r_{t+1} = r_t$.

Define

$$M = c(\alpha_1 P^T + \alpha_2 (P^2)^T), \tag{9}$$

$$N = (1-c)(I - c(\alpha_1 P^T + \alpha_2 (P^2)^T))^{-1}. \tag{10}$$

Thus, using (9) and (10) we get

$$r_{t+1} - N r_0 = M(r_t - N r_0). \tag{11}$$

Define

$$B_t = r_t - N r_0. \tag{12}$$

Then

$$B_{t+1} = M B_t. \tag{13}$$

By (13), when t = 0, we have $B_0 = (I-N) r_0$, thus

$$B_t = M^t (I-N) r_0, \tag{14}$$

$$r_t = [N + M^t (I-N)] r_0. \tag{15}$$

Since $\lim_{t\to\infty} M^t = 0$, we have

$$\lim_{t\to\infty} r_t = N r_0 = (1-c)(I - c(\alpha_1 P^T + \alpha_2 (P^2)^T))^{-1} r_0. \tag{16}$$

Hence,

$$\lim_{t\to\infty} r_{t+1} - r_t = 0, \tag{17}$$

which implies the convergence of the algorithm is proved.

2.2.5.3 2hop-connectivity feature score

Any two nodes can be ranked twice according to 2hopRWR. Define $\Pi = \{\pi_{ij}\}_{|V|\times|V|}$ be the stable probability matrix where π_{ij} indicates the stable probability between node v_i and node v_j, that is, 2hopRWR starts from node v_i and the probability of reaching node v_j when the process is stable. Briefly speaking, the value of π_{ij} is the j-th element of steady-state probability $\lim_{t\to\infty} r_t$ when the i-th element of r_0 is 1. Therefore, define a local feature score S_{2-hop} for node v_i as follows:

$$S_{2-hop}(v_i) = \sum_{j=1}^{|V|} \pi_{ij} \tag{18}$$

2.3 Global feature

In this paper, we consider integrating local features to get a new network index: global feature.

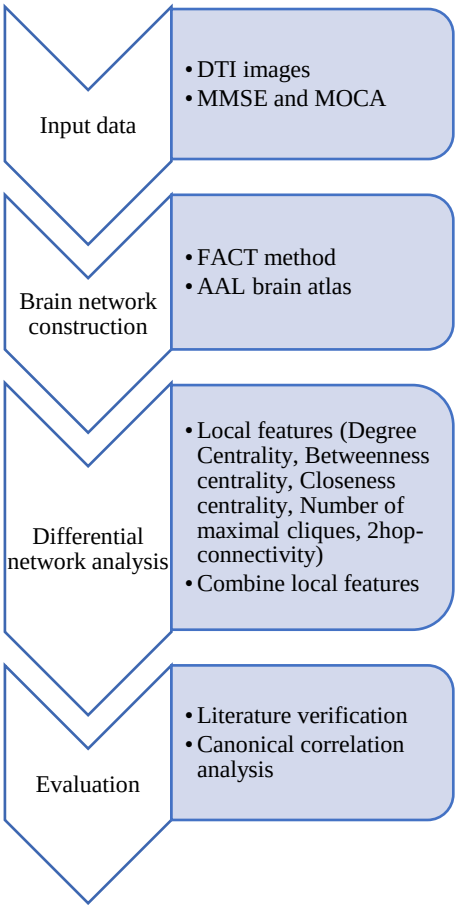

Fig.3 Workflow of our approach.

We normalized the component of different feature scores to [0, 1]. The normalized features are recorded as NC_D, NC_B, NC_C, NN_{MC}, and NS_{2-hop}.

Then, define global feature score GFS for node v_i as follows:

$$GFS(v_i) = \frac{1}{5}[NC_D(v_i) + NC_B(v_i) + NC_C(v_i) + NN_{MC}(v_i) + NS_{2-hop}(v_i)] \tag{19}$$

If the GFS of a node is relatively high, it means that the node plays a key role in the network.

3. Results

3.1 Top 10 brain regions for literature verification

By comparing the GFS of the non-AD group with that of the AD group, we got the top ten brain regions in GFS scoring difference (that is, $GFS_{non-AD}(v_i) - GFS_{AD}(v_i)$). Then, literature verification was carried out to find out whether these brain regions are related to AD, and the

results are as follows:

Table 1 Top ten brain regions in GFS scoring difference between AD and non-AD groups.

Rank	Region ID	AAL regions	Evidence
1	40	ParaHippocampal_R	(van Hoesen *et al.*, 2000)
2	3	Frontal_Sup_L	(Perri *et al.*, 2005)
3	37	Hippocampus_L	(Du *et al.*, 2001)
4	42	Amygdala_R	(Tsuchiya and Kosaka, 1990)
5	22	Olfactory_R	(Wilson *et al.*, 2009)
6	78	Thalamus_R	(Ryan *et al.*, 2013)
7	15	Frontal_Inf_Orb_L	(Salat *et al.*, 2001)
8	9	Frontal_Mid_Orb_L	(Salat *et al.*, 2001)
9	68	Precuneus_R	(Karas *et al.*, 2007)
10	38	Hippocampus_R	(Du *et al.*, 2001)

For the brain structure network of AD group and non-AD group, the visualization results (Manning *et al.*, 2014) show that the top 10 brain regions are relatively concentrated, as shown in Fig. 4 and Fig. 5.

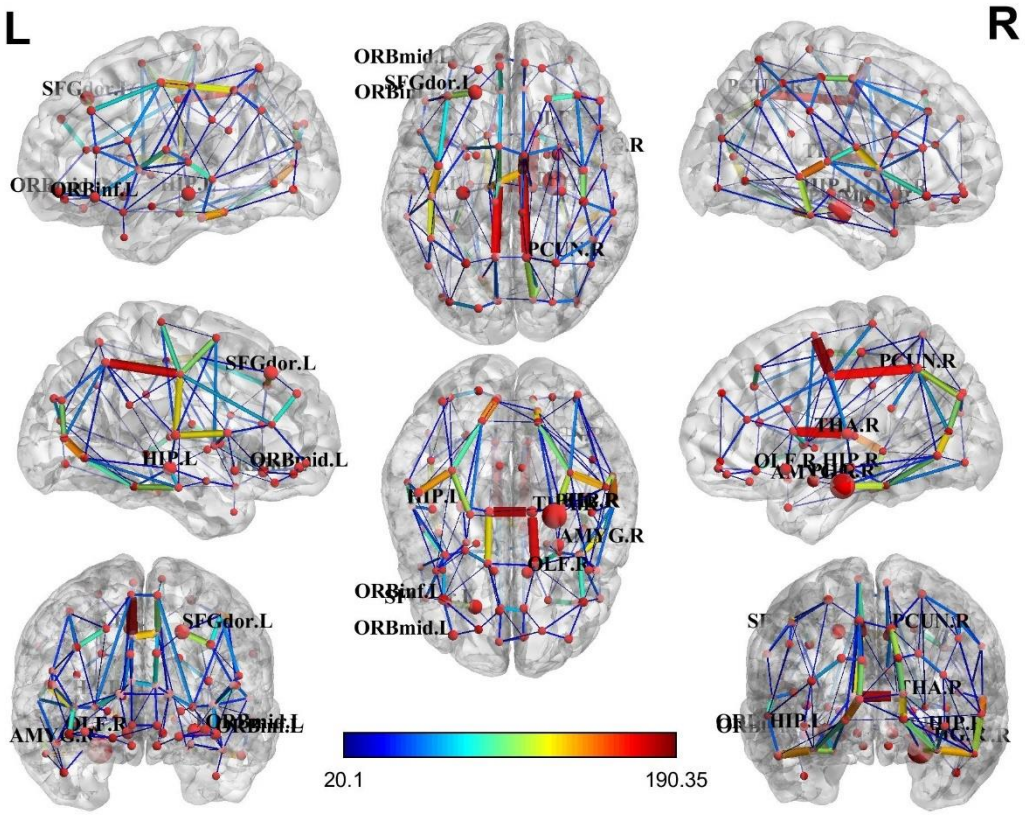

Fig.4 Brain structural network of AD group.

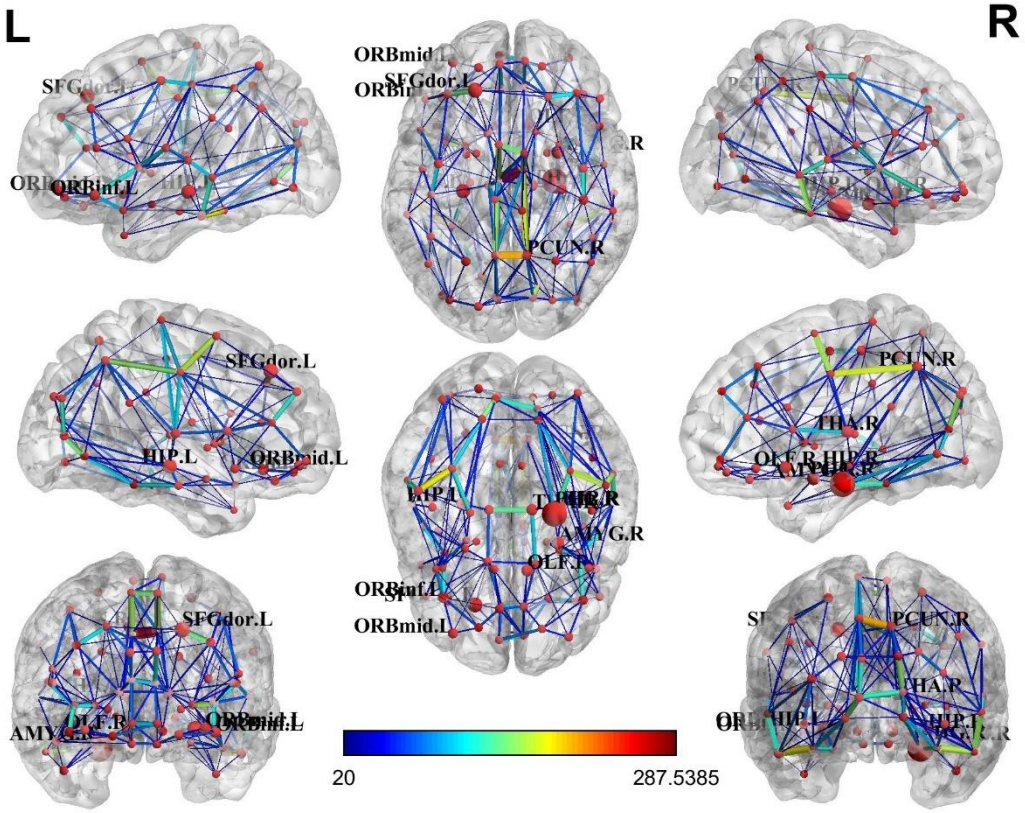

Fig.5 Brain structural network of non-AD group.

3.2 Canonical correlation analysis

In this section, we analyzed whether the GFS for Top 10 brain regions is related to the results of MMSE and MoCA. It can analyze whether there is a correlation between two groups of variables. Because some of the people were illiterate, they could not complete the MoCA test, so we took all the people who completed the two scales, a total of 29 people (19 AD and 10 non-AD). At this time, the canonical correlation analysis can be used. Its basic principle is: to grasp the correlation between the two groups of variables as a whole, two composite variables U and V (linear combination of each variable in the two groups) are extracted from the two groups of variables respectively, and the correlation between the two composite variables is used to reflect the overall correlation between the two groups of variables.

The results of the canonical correlation analysis showed that the correlation coefficient between the typical variable pair 1 is 0.7136, which means that there is a very close correlation between GFS and MMSE/MOCA scale information.

4. Discussion

In this paper, we set a new local feature index 2hop-connectivity to measure the correlation among different areas. And for this, a novel random walk algorithm, 2hopRWR, is proposed, which can compute the local feature index 2hop-connectivity. At the same time, the proof of convergence is given. If there is a lack of edge in the network, it may be more reasonable to use 2hopRWR to analyze the associations between nodes. Next, this paper used the idea of combining 5 local properties to obtain the global feature score (GFS), which is more persuasive than using a single network parameter to describe the importance of network nodes. Then, the results of literature

verification and canonical correlation analysis also validate the reasonableness and effectiveness of the proposed method. Therefore, GFS can be used to distinguish DTI images of the AD group and the non-AD group. Finally, all the top ten brain regions in the GFS scoring difference predicted in this paper have been verified by literature.

Despite the effectiveness of our work, it also has several limitations. First of all, the mechanism of combining local features is relatively simple. For formula (19), we simply think that the weight of each property is the same, if we can combine more effective information, we can use more reasonable weight distribution to have a deeper understanding of the structure and function network of the brain. Secondly, the brain network constructed in this paper is a structural network, which should be combined with structure and function in the future. For example, if we combine the fMRI data with the existing data to analyze the differences of different brain regions in different tasks, we may get more results.

In brief, GFS is expected to be an important and useful index for identifying the difference between network nodes and detecting the changes in information transmission between brain regions in Alzheimer's disease patients. Moreover, it may provide useful insights into the underlying mechanisms of Alzheimer's disease. Finally, GFS can be used as a differential network analysis method (Lichtblau *et al.*, 2017) in other areas of network analysis. We also look forward to the application of the 2hopRWR algorithm in traditional network analysis tasks, such as node classification, link prediction, graph classification.

References

Cui, Z. *et al.* (2013) PANDA: a pipeline toolbox for analyzing brain diffusion images. *Frontiers in human neuroscience*, **7**, 42.

Du, A.T. *et al.* (2001) Magnetic resonance imaging of the entorhinal cortex and hippocampus in mild cognitive impairment and Alzheimer's disease. *Journal of neurology, neurosurgery, and psychiatry*, **71**, 441–447.

Fan, L. *et al.* (2016) The Human Brainnetome Atlas: A New Brain Atlas Based on Connectional Architecture. *Cereb. Cortex*, **26**, 3508–3526.

John, M., Ikuta, T. and Ferbinteanu, J. (2016) Graph analysis of structural brain networks in Alzheimer's disease.

Karas, G. *et al.* (2007) Precuneus atrophy in early-onset Alzheimer's disease: a morphometric structural MRI study. *Neuroradiology*, **49**, 967–976.

Lichtblau, Y. *et al.* (2017) Comparative assessment of differential network analysis methods. *Briefings in bioinformatics*, **18**, 837–850.

Liu, J. *et al.* (2017) Complex Brain Network Analysis and Its Applications to Brain Disorders: A Survey. *Complexity*, **2017**, 1–27.

Manning, J.R. *et al.* (2014) Topographic factor analysis: a Bayesian model for inferring brain networks from neural data. *PLoS ONE*, **9**, e94914.

Perri, R. *et al.* (2005) Alzheimer's disease and frontal variant of frontotemporal dementia-- a very brief battery for cognitive and behavioural distinction. *Journal of neurology*, **252**, 1238–1244.

Ryan, N.S. *et al.* (2013) Magnetic resonance imaging evidence for presymptomatic change in

thalamus and caudate in familial Alzheimer's disease. *Brain : a journal of neurology*, **136**, 1399–1414.

Salat, D.H. *et al.* (2001) Selective preservation and degeneration within the prefrontal cortex in aging and Alzheimer disease. *Archives of neurology*, **58**, 1403–1408.

Sanz-Arigita, E.J. *et al.* (2010) Loss of 'Small-World' Networks in Alzheimer's Disease: Graph Analysis of fMRI Resting-State Functional Connectivity. *PLoS ONE*, **5**, e13788.

Tong, H. *et al.* (2006 - 2006) Fast Random Walk with Restart and Its Applications. In, Sixth International Conference on Data Mining (ICDM'06). IEEE, 613–622.

Tsuchiya, K. and Kosaka, K. (1990) Neuropathological study of the amygdala in presenile Alzheimer's disease. *Journal of the Neurological Sciences*, **100**, 165–173.

van Hoesen, G.W. *et al.* (2000) The parahippocampal gyrus in Alzheimer's disease. Clinical and preclinical neuroanatomical correlates. *Annals of the New York Academy of Sciences*, **911**, 254–274.

Wilson, R.S. *et al.* (2009) Olfactory impairment in presymptomatic Alzheimer's disease. *Annals of the New York Academy of Sciences*, **1170**, 730–735.

- Ethics approval and consent to participate

Not applicable.

- Consent to publish

Not applicable.

- Competing interests

The authors declare that they have no competing interests.

- Funding

The authors thank all study participants for their participation.

This work was supported by National Natural Science Foundation of China under Grant No. 11631014.and National Key R&D Program of China (2018YFC1314200).